Down-regulation of neurosteroid biosynthesis in corticolimbic circuits mediates social isolation-induced behavior in mice

Roberto C. Agís-Balboa, Graziano Pinna, Fabio Pibiri, Bashkim Kadriu, Erminio Costa*, and Alessandro Guidotti

Psychiatric Institute, Department of Psychiatry, School of Medicine, University of Illinois at Chicago, 1601 West Taylor Street, Chicago, IL 60612

Contributed by Erminio Costa, October 3, 2007 (sent for review June 12, 2007)

Allopregnanolone (ALLO), synthesized by pyramidal neurons, is a potent positive allosteric modulator of the action of GABA at $GABA_A$ receptors expressing specific neurosteroid binding sites. In the brain, ALLO is synthesized from progesterone by the sequential action of two enzymes: 5α-reductase type I (5α-RI) and 3α-hydroxysteroid dehydrogenase (3α-HSD). In the cortex, hippocampus, and amygdala, these enzymes are colocalized in principal glutamatergic output neurons [Agís-Balboa RC, Pinna G, Zhubi A, Maloku E, Veldic M, Costa E, Guidotti A (2006) *Proc Natl Acad Sci USA* 103:14602–14607], but they are not detectable in GABAergic interneurons. Using RT-PCR and *in situ* hybridization, this study compares 5α-RI and 3α-HSD mRNA brain expression levels in group housed and in socially isolated male mice for 4 weeks. In these socially isolated mice, the mRNA expression of 5α-RI was dramatically decreased in hippocampal CA3 glutamatergic pyramidal neurons, dentate gyrus granule cells, glutamatergic neurons of the basolateral amygdala, and glutamatergic pyramidal neurons of layer V/VI frontal (prelimbic, infralimbic) cortex (FC). In contrast, 5α-RI mRNA expression failed to change in CA1 pyramidal neurons, central amygdala neurons, pyramidal neurons of layer II/III FC, ventromedial thalamic nucleus neurons, and striatal medium spiny and reticular thalamic nucleus neurons. Importantly, 3α-HSD mRNA expression was unchanged by protracted social isolation (*Si*). These data suggest that, in male mice, after 4 weeks of *Si*, the expression of 5α-RI mRNA, which is the rate-limiting-step enzyme of ALLO biosynthesis, is specifically down-regulated in glutamatergic pyramidal neurons that converge on the amygdala from cortical and hippocampal regions. In socially isolated mice, this down-regulation may account for the appearance of behavioral disorders such as anxiety, aggression, and cognitive dysfunction.

5α-reductase | amygdala | glutamatergic neurons | allopregnanolone | aggression

The neurosteroid 3α-hydroxy-5α-pregnan-20-one [allopregnanolone (ALLO)] is a potent positive allosteric modulator of the action of GABA at $GABA_A$ receptors (1, 2). This neurosteroid is synthesized in the brain from progesterone (3) by the sequential action of two enzymes: 5α-reductase type I (5α-RI), which transforms progesterone into 5α-dihydroprogesterone (5α-DHP), and 3α-hydroxysteroid dehydrogenase (3α-HSD), which converts 5α-DHP into ALLO (4). In the cortex, hippocampus, amygdala, thalamus, and olfactory bulb, 5α-RI and 3α-HSD colocalize in principal output glutamatergic neurons characterized by the expression of vesicular glutamate transporter 2 (VGLUT2) but are not expressed in GABAergic [glutamic acid decarboxylase 65/67 (GAD65/67)-positive] interneurons (5). Taken together, these data suggest that ALLO synthesized in cortical, hippocampal, thalamic, or amygdaloid glutamatergic principal neurons may modulate the action of GABA at $GABA_A$ receptors, by an autocrine or a paracrine mechanism (2, 5) or by a mechanism that allows ALLO to reach $GABA_A$ receptor sites via lateral membrane diffusion (6, 7).

In male mice, 3–4 weeks of social isolation (*Si*) elicit a marked (≈50%) decrease of ALLO levels in the cortex and olfactory bulb (8, 9); this decrease has been attributed to a selective down-regulation of 5α-RI expression because it occurs in the absence of changes in 3α-HSD mRNA expression (9).

It is well known that, in male mice, *Si* not only may affect several biochemical and behavioral functions (10–13) but also may even change drug susceptibility. For example, mice socially isolated for 4 weeks show altered responsiveness to barbiturates, benzodiazepines, and other GABA-mimetic drugs (8, 14). Behaviorally, these mice become emotionally unstable, showing (*i*) aggressiveness toward an intruder, (*ii*) increased locomotor activity in a novel environment, and (*iii*) an increased intensity of fear conditioning (F.P., unpublished data). It has been suggested that the neuronal pathways that underlie aggression, anxiety, and fear conditioning expression include neuronal networks that comprise excitatory glutamatergic projections from the frontal (prelimbic and infralimbic) cortex (FC), hippocampus (Fig. 1*A*), and thalamus to the basolateral nuclei of the amygdala (BLA) (15–20). In the BLA, the cortical and hippocampal projections establish excitatory synapses with the pyramidal-like glutamatergic output neurons, which in turn project to the intercalated (ITC) inhibitory GABAergic neurons located on the capsule division of the central amygdaloid nucleus (CeA) (Fig. 1*A*). Hence, via ITC GABAergic neurons, the FC and hippocampus establish an inhibitory control over the CeA GABAergic spiny output neurons, which in turn project to the brainstem and hypothalamus, thereby influencing *inter alia* the intensity of emotional responses to environmental stimuli (Fig. 1*A*).

The present article deals with our attempt to identify the corticolimbic, corticostriatal, or corticothalamic neuronal circuits exhibiting a decrease of 5α-RI in the brain of mice socially isolated for 4 weeks. Our study demonstrates that 5α-RI is specifically down-regulated in glutamatergic neurons of corticolimbic structures, such as hippocampus CA3, the dentate gyrus (DG), BLA, and FC layers V/VI. In addition, after *Si*, the 5α-RI expression fails to change in principal GABAergic neurons of the striatum and reticular thalamic nucleus (RtN). It is interesting that, after *Si*, 3α-HSD remained unchanged.

Results

Expression of 5α-RI and 3α-HSD mRNA in Different Brain Regions of Group Housed and Socially Isolated Mice. ***Quantitative RT-PCR.*** Table 1 shows that, in mice socially isolated for 4 weeks, the expression of 5α-RI mRNA is down-regulated in the FC, hippocampus, and amygdala but not in the striatum compared with group housed mice. In contrast, the expression of 3α-HSD mRNA fails to change.

Author contributions: R.C.A.-B., G.P., F.P., E.C., and A.G. designed research; R.C.A.-B. and F.P. performed research; R.C.A.-B., F.P., and B.K. analyzed data; and R.C.A.-B., G.P., E.C., and A.G. wrote the paper.

The authors declare no conflict of interest.

*To whom correspondence should be addressed. E-mail: ecosta@psych.uic.edu.

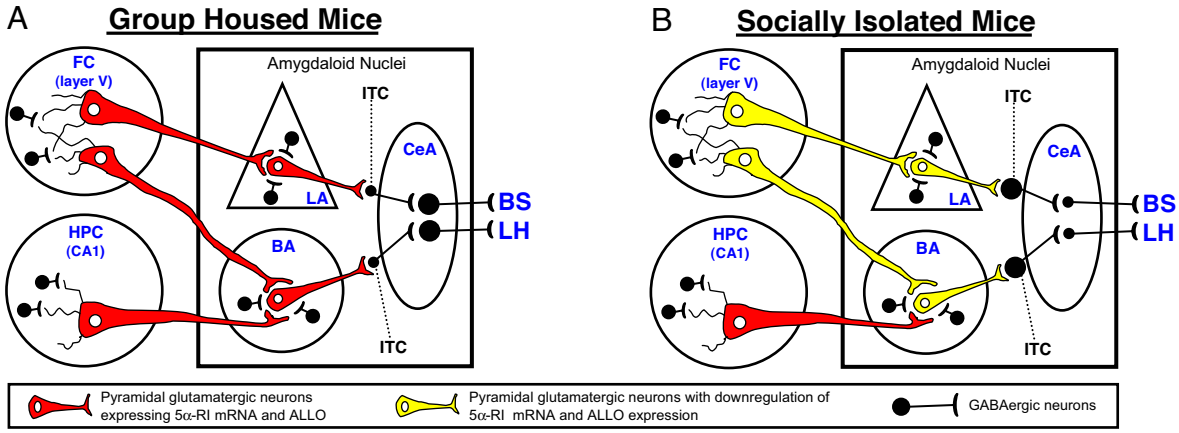

Fig. 1. In socially isolated mice, a decrease in ALLO biosynthesis in FC and BLA principal glutamatergic neurons down-regulates the inhibitory potency of GABAergic interneurons. Shown is a schematic summary of the main intrinsic connections of the nuclei of the amygdala and the extrinsic cortical (layer V pyramidal neurons) and hippocampal (CA1 pyramidal neurons) inputs. Note that the expression of 5α-RI mRNA and ALLO in FC pyramidal glutamatergic neurons and in pyramidal-like glutamatergic neurons intrinsic to the BLA (neurons color-coded in red in *A*) show a marked reduction in socially isolated mice (neurons color-coded in yellow in *B*). The decrease of ALLO in FC and BLA pyramidal neurons will reduce the inhibitory potency of GABA released from local GABAergic interneurons. BA, basal amygdaloid nucleus; BS, brainstem; HPC, hippocampus; ITC, intercalated GABAergic neurons (do not express 5α-RI mRNA; see Fig. 7); LA, lateral amygdaloid nucleus; LH, lateral hypothalamus. [Modified from Sah *et al.* (15) and Sotres-Bayon *et al.* (16).]

In situ *hybridization: FC.* Here we define FC as the brain region located 1.9 to 1.4 mm anterior to bregma (21) and including the cingulate, prelimbic, and infralimbic cortices.

Fig. 2 shows that, in the FC of the group housed mice, 5α-RI mRNA and protein are expressed in cell bodies and dendrites of glutamatergic (VGLUT2 protein-positive) pyramidal neurons. We have previously reported that, in pyramidal neurons, 5α-RI colocalizes with 3α-HSD and that 5α-RI and 3α-HSD mRNAs are undetectable in GAD65/67-positive interneurons (5).

Fig. 3 shows the 5α-RI mRNA *in situ* hybridization signal in FC layer V pyramidal neurons of group housed mice. After 4 weeks of *Si*, the intensity of 5α-RI mRNA staining is specifically decreased in these neurons. Overall, there is a 37% decrease in the intensity of the 5α-RI *in situ* hybridization signal in FC layer V/VI pyramidal neurons of socially isolated mice (Fig. 4*A*). However, this signal fails to change in layer II/III pyramidal neurons (Fig. 4*A*). Neither the FC pyramidal neurons of layer II/III nor those of layer V/VI show significant changes in 3α-HSD mRNA detected with *in situ* hybridization after 4 weeks of *Si* (Figs. 3 and 4*B*).

In situ *hybridization: Hippocampal formation.* In CA1/CA3 pyramidal neurons and in DG granule cells, 5α-RI mRNA and VGLUT2 are colocalized (Fig. 5).

After protracted *Si* the intensity of the 5α-RI mRNA *in situ* hybridization signal is decreased by 75% in CA3 glutamatergic pyramidal neurons and by 68% in DG glutamatergic granule cells (Figs. 4*A* and 6). However, the expression of 5α-RI mRNA in CA1 glutamatergic pyramidal neurons fails to change (Fig. 4*A*). 3α-HSD mRNA colocalizes with 5α-RI mRNA in CA1/CA3 pyramidal neurons and in DG granule cells (5). However, 3α-HSD mRNA appears to be unaffected after protracted *Si* in every area studied; only a slight decrease (25%) appears in DG granule cells (Fig. 4*B*).

In situ *hybridization: Amygdaloid nuclei.* A strong expression of the *in situ* hybridization signal for 5α-RI mRNA is present in "pyramidal-like" neurons of the BLA whereas this signal is weaker in neurons of the CeA nucleus (Fig. 7). The pyramidal-like neurons of the BLA show a colocalization of 5α-RI mRNA with VGLUT2 proteins (Fig. 7 *C1–C3*). In addition, in the BLA, 5α-RI mRNA fails to colocalize with GAD65/67 proteins (Fig. 7 *D1–D3*).

Figs. 4*A* and 6 show that, after protracted *Si*, the 5α-RI mRNA

Table 1. 5α-RI and 3α-HSD mRNA levels in various brain areas of male mice group housed or socially isolated for 4 weeks

	5α-RI mRNA		3α-HSD mRNA	
Brain area	Group housed	Socially isolated	Group housed	Socially isolated
FC	12 ± 1.7	5.1 ± 1.2*	12 ± 2.4	11 ± 2.9
Amygdala	4.2 ± 0.5	2.6 ± 0.5*	12 ± 1	10 ± 2
Hippocampus	5.8 ± 0.6	3.5 ± 0.6*	8.6 ± 1.1	8.9 ± 1.4
Striatum	8 ± 1	7.1 ± 2	8.8 ± 1.2	9.8 ± 0.9

5α-RI and 3α-HSD mRNAs are expressed in femtomoles of 5α-RI or 3α-HSD mRNA per picomole of NSE mRNA. Each value represents the mean ± SE of five mice. *, $P < 0.05$ (Student's *t* test) when socially isolated mice were compared with group housed mice.

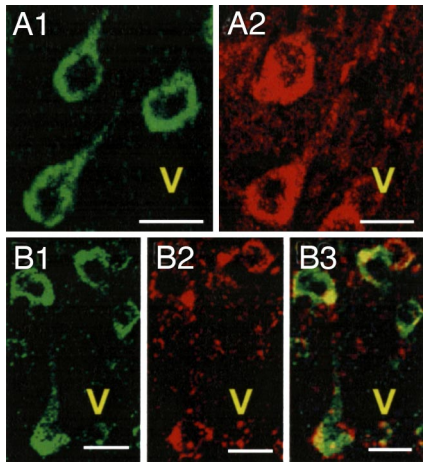

Fig. 2. 5α-RI mRNA is expressed in glutamatergic neurons of FC. (*A1*) Confocal image of 5α-RI mRNA in FC layer V (V) pyramidal neurons color-coded in green. (*A2*) 5α-RI protein in FC layer V pyramidal neurons color-coded in red. (*B1*) 5α-RI mRNA in FC layer V pyramidal neurons color-coded in green. (*B2*) VGLUT2 protein in the same neurons color-coded in red. (*B3*) Merge of *B1* and *B2*. Coronal sections correspond roughly to bregma +1.4 mm (21). (Scale bars: 20 μm.)

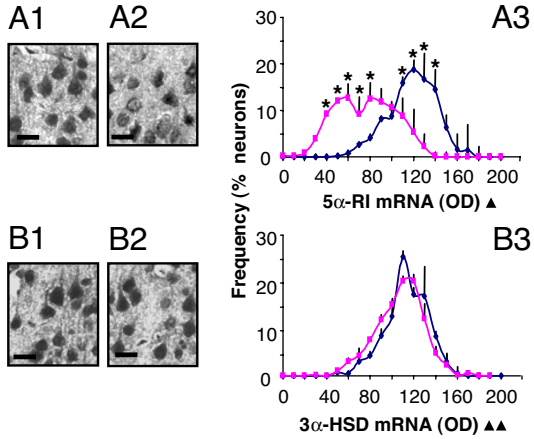

Fig. 3. 5α-RI (*A1–A3*) but not 3α-HSD (*B1–B3*) mRNA is specifically down-regulated in layer V pyramidal neurons of the FC of socially isolated mice. (*A1* and *B1*) Photomicrographs of 5α-RI (*A1*) and 3α-HSD (*B1*) mRNA *in situ* hybridization DAB staining in FC layer V pyramidal neurons of group housed mice. (*A2*) The intensity of the 5α-RI mRNA *in situ* hybridization signal is markedly decreased in FC layer V pyramidal neurons of socially isolated mice. (*B2*) The 3α-HSD mRNA *in situ* hybridization signal remains unchanged after *Si*. (*A3* and *B3*) Compare the densitometric (OD) distribution profiles of the 5α-RI (*A3*) and 3α-HSD (*B3*) mRNA *in situ* hybridization signals in group housed mice (blue traces) and in socially isolated mice (pink traces). Note a shift to the left in the intensity of the 5α-RI *in situ* hybridization signal in FC layer V pyramidal neurons of socially isolated mice. ▲, 5α-RI mRNA (OD) refers to the relative intensity of the 5α-RI *in situ* hybridization signal; ▲▲, 3α-HSD mRNA (OD) refers to the relative intensity of the 3α-HSD *in situ* hybridization signal. For densitometric distribution profiles, each point is the mean ± SE of five mice. *, statistically significant differences among group housed and socially isolated mice ($P < 0.05$) when the data are analyzed by two-way repeated-measures ANOVA followed by a Student–Newman–Keuls multiple-comparison test. The coronal section is as in Fig. 2. (Scale bars: 25 μm.)

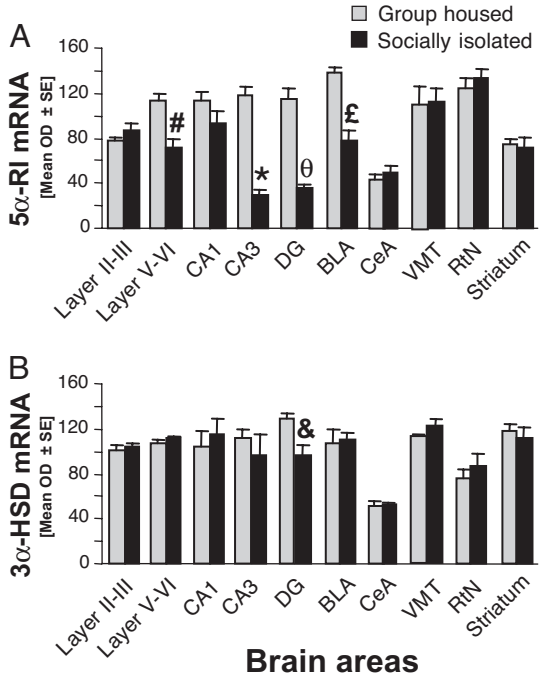

Fig. 4. 5α-RI (*A*) and 3α-HSD (*B*) mRNA expression in corticolimbic regions of group housed and socially isolated mice: *in situ* hybridization studies. Each bar represents the mean OD ± SE of 5α-RI or the 3α-HSD mRNA *in situ* hybridization signal in neurons of various corticolimbic structures. Results from five mice either group housed or socially isolated for 4 weeks. #, $P < 0.01$ (37% decrease); *, $P < 0.001$ (75% decrease); θ, $P < 0.001$ (68% decrease); £, $P < 0.002$ (44% decrease); &, $P < 0.05$ (25% decrease) (versus respective group housed mice; Student's *t* test). Layer II/III, layers II/III of FC; Layer V/VI, layers V/VI of FC; CA1, hippocampal CA1 pyramidal layer; CA3, hippocampal CA3 pyramidal layer.

expression level is significantly decreased (44%) in glutamatergic neurons of the BLA. However, in the same mice 3α-HSD mRNA levels are unchanged (Fig. 4*B*). Neither 5α-RI nor 3α-HSD mRNA expression is altered in the CeA by *Si* (Fig. 4).

In situ *hybridization: Striatum.* Approximately 95% of striatal neurons are medium spiny GABAergic neurons that express 5α-RI mRNA (Fig. 6). Protracted *Si* fails to alter the *in situ* hybridization signals of either 5α-RI (Figs. 4*A* and 6) or 3α-HSD (Fig. 4*B*) mRNAs.

In situ *hybridization: Thalamus.* The ventromedial thalamic nucleus (VMT) contains glutamatergic neurons that express strong 5α-RI and 3α-HSD mRNA *in situ* hybridization signals (Fig. 4). The RtN almost exclusively includes principal GABAergic neurons that also express strong 5α-RI and 3α-HSD mRNA *in situ* hybridization signals (5). Protracted *Si* does not affect the 5α-RI or 3α-HSD mRNA signal intensity in either VMT or RtN (Fig. 4).

Neuronal counts. By using a specific marker for neuronal nuclear proteins (NeuN), neuronal counts were performed in the hippocampus CA3 layer, DG, and BLA. The number of positive NeuN neurons is similar in group housed and socially isolated animals (Student's *t* test). These counts are expressed as the mean (number of neurons per square millimeter) ± SE (GH and SI signify group housed and socially isolated, respectively): DG_{GH}, 2,225 ± 169; DG_{SI}, 2,050 ± 64 ($P = 0.372$); $CA3_{GH}$, 454 ± 15; $CA3_{SI}$, 441 ± 56 ($P = 0.824$); BLA_{GH}, 280 ± 10; BLA_{SI}, 257 ± 9 ($P = 0.181$).

Discussion

In Socially Isolated Mice, a Down-Regulation of 5α-RI mRNA Is Expressed Along Well Defined Brain Structure Boundaries. A major finding of this study is that, in mice, *Si* induces a marked down-regulation (≈50%) of 5α-RI mRNA expression in selected neuronal populations of the hippocampus, amygdala, and cortex (schematically shown in Fig. 1*B*).

A histological examination reveals that there is a 65–75% decrease of 5α-RI mRNA levels in CA3 glutamatergic pyramidal neurons and in DG granule cells and a 40–50% decrease of mRNA levels in BLA glutamatergic output neurons. There is

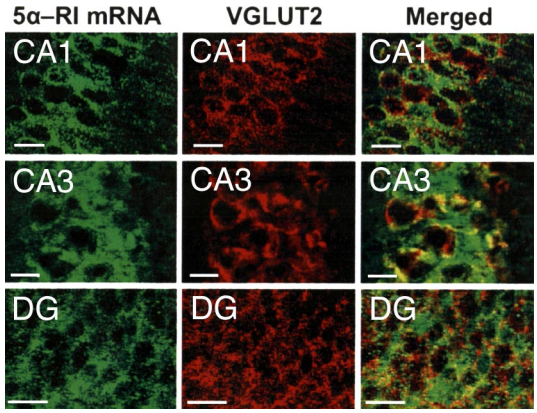

Fig. 5. 5α-RI mRNA is coexpressed with VGLUT2 (a glutamatergic marker) in CA1, CA3 pyramidal, and DG granule neurons of the hippocampal formation. (*Left*) Confocal images of 5α-RI mRNA-positive neurons coded in green. (*Center*) VGLUT2 protein-immunopositive neurons coded in red. (*Right*) Merge. The coronal section corresponds roughly to bregma −2.46 mm (21). (Scale bars: 20 μm.)

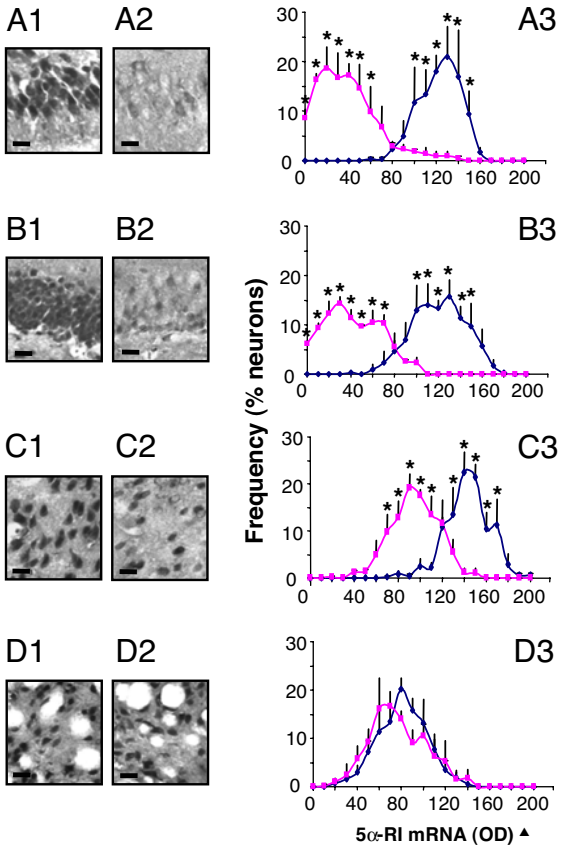

Fig. 6. 5α-RI mRNA is specifically down-regulated in CA3, DG, and BLA glutamatergic output neurons but not in striatal medium spiny GABAergic neurons of socially isolated mice. (*A1–D1*) Photomicrographs of 5α-RI mRNA *in situ* hybridization DAB staining in CA3 pyramidal neurons (*A1*), DG granule cells (*B1*), glutamatergic pyramidal-like neurons of the BLA neurons (*C1*), and GABAergic (GAD65/67-positive) medium spiny neurons of the striatum (*D1*) of group housed mice. (*A2–D2*) The intensity of the 5α-RI mRNA *in situ* hybridization signal is dramatically decreased in CA3 (*A2*), DG (*B2*), and BLA (*C2*) glutamatergic neurons, but not in GABAergic medium spiny neurons of the striatum (*D2*) of socially isolated mice. (*A3–D3*) Compare the densitometric (OD) distribution profiles of the 5α-RI mRNA *in situ* hybridization signal in CA3 (*A3*), DG (*B3*), BLA (*C3*), and striatum (*D3*) of group housed mice (blue traces) and socially isolated mice (pink traces). Note a shift to the left in the intensity of the 5α-RI *in situ* hybridization signal in CA3 pyramidal neurons, DG granule cells, and BLA glutamatergic neurons, but not in GABAergic medium spiny neurons of the striatum of socially isolated mice. (*A1–A3* and *B1–B3*) Coronal sections are as in Fig. 5. (*C1–C3*) Coronal sections correspond roughly to bregma −1.58 mm (21). (*D1–D3*) Coronal sections correspond roughly to bregma +1.10 mm (21). ▲, 5α-RI mRNA (OD) refers to the relative intensity of the 5α-RI *in situ* hybridization signal. For densitometric distribution profiles, each point is the mean ± SE of five mice. *, statistically significant differences between group housed and socially isolated mice ($P < 0.05$) when the data were analyzed by two-way repeated-measures ANOVA followed by a Student–Newman–Keuls multiple-comparison test. (Scale bars: 25 μm.)

also a smaller (≈35%) decrease in FC layer V/VI glutamatergic pyramidal neurons. Interestingly, a decrease of 5α-RI mRNA levels in FC layers II/III, hippocampal CA1 layer pyramidal neurons, CeA neurons, or VMT neurons could not be detected. Furthermore, the 5α-RI mRNA levels in GABAergic output neurons, such as medium spiny neurons of striatum and RtN neurons, fail to change. In addition, in the same glutamatergic neurons in which 5α-RI mRNA is decreased the 3α-HSD mRNA levels remained unchanged. These data suggest that the decrease of 5α-RI mRNA expression in CA3, DG, BLA, and FC (layer V/VI) of socially isolated mice is not related to generalized

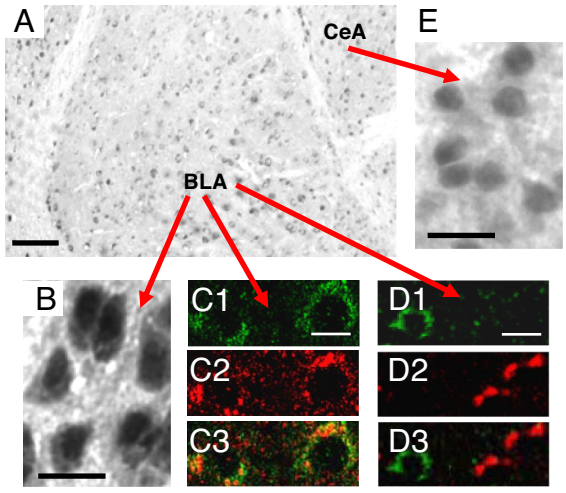

Fig. 7. In the BLA, 5α-RI mRNA is expressed in glutamatergic but not in GABAergic neurons. (*A*) Photomicrograph showing a strong *in situ* hybridization DAB staining for 5α-RI expressed in the pyramidal-like neurons of the BLA (*A* and *B*), whereas in the CeA the same staining is weaker (*A* and *E*). The coronal section is as in Fig. 6 *C1–C3*. (*C1*) Confocal image of 5α-RI mRNA-positive neurons in the BLA coded in green. (*C2*) VGLUT2-immunopositive neurons coded in red. (*C3*) Merge of *C1* and *C2*. The coronal section is as in Fig. 6 *C1–C3*. (*D1*) Confocal image of 5α-RI mRNA-positive neurons in the BLA coded in green. (*D2*) GAD65/67-immunopositive neurons coded in red. (*D3*) Merge of *D1* and *D2*. The coronal section is as in Fig. 6 *C1–C3*. [Scale bars: 100 μm (*A*) and 20 μm (*B–E*).]

neurotoxicity or to a generalized down-regulation of gene expression because 3α-HSD mRNA remains unchanged and the number of NeuN-positive neurons fails to change in the same brain regions.

Is the Down-Regulation of 5α-RI Expression in Selected Corticolimbic Neuronal Populations Operative in the Spectrum of Behavioral Alterations Detected in Socially Isolated Mice? The amygdaloid nuclear complex, which receives sensory inputs from the cortex, hippocampus (Fig. 1*A*), and thalamus, is critical to recruit appropriate emotional behavioral responses to sensory afferent stimuli (15–19).

Here we will consider how the reduction of GABA action at $GABA_A$ receptors elicited by the down-regulation of ALLO biosynthesis in specific cortical, hippocampal, or amygdaloid glutamatergic neurons of socially isolated mice may disrupt the function of the (*i*) FC–amygdaloid and (*ii*) hippocampal–amygdaloid circuits.

Corticoamygdaloid circuit. In the FC of socially isolated mice, layer V/VI pyramidal neurons exhibit a decrease of 5α-RI mRNA expression (Figs. 3 and 4).

Because layer V/VI pyramidal neurons are the main excitatory output of the cerebral cortex (22), a reduction of $GABA_A$ receptor function by a down-regulation of ALLO biosynthesis (8, 10) in these neurons could result in decreased plasticity of the inhibitory regulation and in an indirect activation of the cortical excitatory output. Among the target regions of FC layer V/VI pyramidal neurons of particular interest in explaining the behavioral alterations observed in socially isolated mice appears to be the amygdaloid nuclear complex (Fig. 1*A*) (15–20). In group housed mice, FC layer V/VI pyramidal neurons project to the BLA, where they may synapse on either the excitatory glutamatergic spiny multipolar pyramidal-like neurons or GABAergic interneurons (15, 16), or both. The BLA glutamatergic pyramidal-like neurons, in turn, synapse on ITC GABAergic neurons (Fig. 1*A*) located on the capsule division of the CeA, thus providing an important inhibitory input to CeA GABAergic

spiny neurons that project out of the amygdala (Fig. 1*A*). Through this output pathway, the CeA nuclei control the expression of emotional responses (behavioral, autonomic, and hormonal) by way of inhibitory (GABAergic) projections to the brainstem and hypothalamus (Fig. 1*A*) (15–19, 23).

In socially isolated mice, in addition to a down-regulation of ALLO biosynthesis in FC layer V/VI pyramidal neurons, we noticed a decrease in ALLO biosynthesis in BLA glutamatergic pyramidal-like neurons (Fig. 1*B*). This down-regulation could affect the function of intraamygdaloid neuronal connections, for instance by decreasing the potency of GABA at the $GABA_A$ receptors expressed on dendrites or cell bodies of the glutamatergic pyramidal-like neurons.

Hence, a decrease of ALLO biosynthesis in selected neuronal populations of the corticoamygdaloid circuit could in part explain aggressive behavior, anxiety, and exaggerated fear observed in socially isolated mice.

Hippocampal–amygdaloid circuit. The sensory information processed in various unimodal or polymodal cortical association areas is processed by the hippocampus via the so-called "trisynaptic circuit." This circuit includes the "perforant pathway" originating from layer II pyramidal neurons of the entorhinal cortex synapsing on the DG granule cells and CA3 pyramidal neurons (24–26). The "mossy fibers" are an additional important excitatory pathway reaching the CA3 field originating from DG granule cells (24–29). These axons also synapse with GABAergic interneurons, which modulate CA3 neuronal excitability by a feedback mechanism (26–29). The CA3 is an important station functioning as an autoassociative memory network that transmits information to CA1 pyramidal neurons via the Schaffer collaterals. The CA1 area is the major output structure of the hippocampus and also provides a main excitatory input to the BLA (also see scheme in Fig. 1) (15, 30), thus contributing along with the FC–amygdala circuits to the acquisition and consolidation of spatial memory and to the expression of emotional components elicited by environmental relevant stimuli (15, 30).

In the hippocampal formation of socially isolated mice, DG granule cells and CA3 glutamatergic pyramidal neurons exhibit an important decrease (65–70%) in 5α-RI mRNA expression whereas 5α-RI mRNA expression of CA1 pyramidal neurons fails to change (Figs. 1 and 4). We suggest that in socially isolated mice the decrease in ALLO levels mediated by a decrease in 5α-RI expression in CA3 and DG glutamatergic neurons brings about a decrease in the efficacy of the GABAergic tone impinging on CA3 pyramidal neurons, thus indirectly providing an increased excitatory input to the CA1 pyramidal neurons, which in turn project to the BLA (Fig. 1*B*). This evidence also suggests that an altered action of the hippocampal input to the amygdala may reflect some aspects of the acquisition and consolidation of contextual fear memory generating the emotional behavioral components observed in socially isolated mice (16, 30).

Conclusions

Neuroanatomical and electrophysiological studies of brain circuits regulating emotions (schematically depicted in Fig. 1*A*) suggest that the neuronal pathways that underlie aggression, anxiety, and fear responses include a specific activation of cortical innervations to the amygdala (15–20).

Several lines of evidence suggest that, in socially isolated mice, aggression, anxiety, and fear are associated with a decrease of brain ALLO levels caused by a down-regulation of 5α-RI expression. Drugs such as fluoxetine and norfluoxetine, which increase ALLO brain levels when given in doses 10- to 50-fold lower than those required to inhibit 5-HT reuptake, reduce aggression and anxiety in socially isolated mice. This is probably independent of their 5-HT reuptake inhibition (8, 13).

In situ hybridization measurements of 5α-RI mRNA expression suggest that, in socially isolated mice, a decrease of ALLO biosynthesis occurs in selected neuronal populations. For example, Fig. 1 shows that the expression of ALLO in layer V/VI glutamatergic pyramidal neurons of the FC and in glutamatergic pyramidal-like neurons of the BLA but not in CA1 pyramidal neurons (neurons color-coded in red in Fig. 1*A*) is markedly reduced (neurons color-coded in yellow in Fig. 1*B*) in socially isolated mice.

Because GABAergic interneurons mediate feed-forward and/or feedback inhibition over the principal glutamatergic output neurons in FC and BLA, a selective decrease of ALLO in cortical layer V/VI pyramidal neurons or BLA glutamatergic output neurons may reduce the inhibitory potency of GABA at $GABA_A$ receptors located on dendrites or cell bodies of these principal neurons. In functional terms, this may represent the molecular mechanisms that underlie the decreased plasticity of the corticolimbic pathways converging on the ITC and CeA GABAergic spiny neurons in socially isolated mice, ultimately resulting in an inhibition of the GABAergic output from the CeA projecting to the hypothalamus and brainstem.

Therefore, by impairing the function of corticoamygdaloid circuits, the reduction of 5α-RI and consequently that of the ALLO biosynthesis in glutamatergic neurons of FC and BLA may explain the aggressive behavior and anxiety observed in socially isolated mice.

Materials and Methods

Animals and Tissue Preparation. Adult male Swiss–Webster mice (Harlan), 25- to 30-g body weight, were used in our experiments. Immediately after decapitation, brain hemispheres were dissected along the sagittal axis. The left hemisphere was (*i*) fixed for 72 h in 4% paraformaldehyde and (*ii*) embedded in 30% sucrose in 0.15 M PBS (pH 7.4) at 4°C. The right hemisphere was immediately frozen and cut into 1-mm-thick slices by using a Jacobovitz brain slicer (Zivic Miller). The slices obtained at 0.9–1.9 mm anterior to the bregma (21) were mounted on a coverslip at −4°C, and disks (1.5-mm diameter) were punched out from the striatum and the FC. Similarly, the slices obtained at 1.06–2.06 mm posterior to the bregma were used to punch out disks (1.5-mm diameter) from the dorsal hippocampus and amygdala (comprising basolateral and central amygdala nuclei). A single disk from each area was used for RNA isolation and RT-PCR studies. All of the animal procedures used in our research were approved by the University of Illinois at Chicago Animal Care Committee.

mRNA *in Situ* Hybridization. To visualize 5α-RI mRNA, free-floating 16- to 20-μm coronal sections (21) were incubated for 72 h at 42°C with a mixture of 50 pmol/ml of three antisense oligonucleotide probes: R1 (910–933), R2 (989–1,012), and R3 (1202–1225) (GenBank accession no. NM_175283). To visualize 3α-HSD mRNA, adjacent sections were incubated with two antisense oligonucleotide probes, H1 (526–549) and H2 (804–827) (GenBank accession no. AY730283.1). The oligonucleotide 3′ terminals were labeled with digoxigenin by using the Oligonucleotide Digoxigenin Tailing Kit (Roche Diagnostics). The *in situ* hybridization protocol followed for the avidin–biotin–peroxidase complex method and for the confocal immunofluorescence studies was described by Agís-Balboa *et al.* (5). Double *in situ* hybridization and immunohistochemistry were carried out as described (5).

Analysis of the Intensity of 5α-RI and 3α-HSD mRNA *in Situ* Hybridization Signals. For each brain area (one obtained from group housed mice and one from socially isolated mice), five to six sections (one every four slices) were processed at the same time for *in situ* hybridization with 5α-RI and 3α-HSD antisense probes. The stained cells were visualized by using a ×40 objective lens. For each brain slice, three randomly selected areas were

analyzed. All analyses were carried out in comparable areas (100 × 100 μm) under the same optical and illumination conditions (for example, light intensity was set to 8 on a scale of 1–10, and exposure time was set to 1.5 ms) in a Zeiss MicroImager. Black and white images were digitized and viewed on a computer by using AxioVision software. Staining intensity inside each cell body perimeter was measured by using Scion Image software (Scion); the OD measurement for each cell is the mean gray of pixels inside the perimeter of cell body, with a 256 grayscale as a reference. The OD background of each section was subtracted from the OD measurement of each cell. To graphically represent the cell immunostaining intensity distribution in each section, we divided the OD values included between 0 and 256 grayscale in categories of decimal units. For each brain region studied, we plotted these OD categories against the percentage of cells (frequency) that fell into the specific category.

In preliminary experiments, we established that the OD values of one given area measured under the same illumination conditions for three times with an interval of 1 day among the various measurements gave similar results: average OD ± SE = 87 ± 2.2, 95 ± 2.1, and 92 ± 2.6 in three separate measurements.

NeuN Immunolabeling and Neuronal Counts. To visualize NeuN protein, free-floating 16- to 20-μm coronal sections from both group housed and socially isolated mice were incubated for 3 days with a mouse anti-NeuN antiserum (diluted 1:500; Chemicon), and 3–3′-diaminobenzidine tetrahydrochloride (DAB) staining was performed as described by Rodriguez *et al.* (31).

For each brain area, five to six sections were taken (one every four slices), and the cells were counted with a bidimensional cell counting method (32) at ×40 magnification in a square area of 100 × 100 μm. The NeuN counts were performed blindly in three randomly selected squares in each of the five to six sections; thus, a total of 15–18 squares per sample were counted.

Quantitative RT-PCR of 5α-RI, 3α-HSD, and Neuron-Specific Enolase (NSE) mRNAs. mRNAs were quantified according to the method of Auta *et al.* (33). Internal standards for 5α-RI, 3α-HSD, and NSE were generated by a site-directed mutagenesis using PCR overlapping extensions to introduce a deletion midway between the amplification primers. Primers for 5α-RI were as follows: forward, 685–710; reverse, 1,075–1,109 (GenBank accession no. J05035). Primers for 3α-HSD: forward, 522–555; reverse, 843–876 (GenBank accession no. S57790). Primers for NSE: forward, 382–405; reverse, 769–792 (GenBank accession no. M22349.1). Each primer pair yielded a single band of the correct molecular size after amplification of RNA isolated from the mouse brain tissue.

Digital Photomicrography. DAB (Sigma) staining images were captured by AxioVision 3.1 (Zeiss) and confocal immunofluorescence by using a Leica Confocal Microscope (Leica Microsystems). The final composites were processed by using Photoshop (Adobe Systems) and PowerPoint (Microsoft).

Statistical Analysis. Results are expressed as the mean ± SE. Student's *t* test or two-way repeated-measures ANOVA followed by a Student–Newman–Keuls multiple-comparison test were used. The criterion for significance was $P < 0.05$.

We thank Dr. F. M. Benes (Harvard Medical School, McLean Hospital, Belmont, MA) and Dr. E. J. Nestler (University of Texas Southwestern Medical Center, Dallas, TX) for their constructive criticisms and suggestions in the preparation of the manuscript. This work was supported by National Institute of Mental Health Grants MH5680 (to A.G.) and MH062090 (to E.C.). F.P. was in part supported by a postdoctoral fellowship, "Master and Back," from the Regione Autonoma della Sardegna, Italy.

1. Puia G, Santi MR, Vicini S, Pritchett DB, Purdy RH, Paul SM, Seeburg PH, Costa E (1990) *Neuron* 4:759–765.
2. Herd MB, Belelli D, Lambert JJ (2007) *Pharmacol Ther* 116:20–34.
3. Cheney DL, Uzunov D, Costa E, Guidotti A (1995) *J Neurosci* 15:4641–4650.
4. Karavolas HJ, Hodges DR (1991) in *Neurosteroids and Brain Function*, eds Costa E, Paul SM (Thieme, New York), pp 135–145.
5. Agís-Balboa RC, Pinna G, Zhubi A, Maloku E, Veldic M, Costa E, Guidotti A (2006) *Proc Natl Acad Sci USA* 103:14602–14607.
6. Akk G, Covey DF, Evers AS, Steinbach JH, Zorumski CF, Mennerick S (2007) *Pharmacol Ther* 116:35–57.
7. Li P, Shu HJ, Wang C, Mennerick S, Zorumski CF, Covey DF, Steinbach JH, Akk G (2007) *J Physiol* 584:789–800.
8. Matsumoto K, Uzunova V, Pinna G, Taki K, Uzunov DP, Watanabe H, Mienville JM, Guidotti A, Costa E (1999) *Neuropharmacology* 38:955–963.
9. Dong E, Matsumoto K, Uzunova V, Sugaya I, Takahata H, Nomura H, Watanabe H, Costa E, Guidotti A (2001) *Proc Natl Acad Sci USA* 98:2849–2854.
10. Puia G, Mienville JM, Matsumoto K, Takahata H, Watanabe H, Costa E, Guidotti A (2003) *Neuropharmacology* 44:49–55.
11. Valzelli L (1981) *Int Pharmacopsychiatry* 16:39–48.
12. Matsumoto K, Puia G, Dong E, Pinna G (2007) *Stress* 10:3–12.
13. Pinna G, Costa E, Guidotti A (2006) *Psychopharmacology (Berlin)* 186:362–372.
14. Pinna G, Agís-Balboa RC, Zhubi A, Matsumoto K, Grayson DR, Costa E, Guidotti A (2006) *Proc Natl Acad Sci USA* 103:4275–4280.
15. Sah P, Faber ES, Lopez De Amentia M, Power J (2003) *Physiol Rev* 83:803–834.
16. Sotres-Bayon F, Bush DE, LeDoux JE (2004) *Learn Mem* 11:525–535.
17. Amaral DG, Insausti R (1992) *Exp Brain Res* 88:375–388.
18. McDonald AJ (1998) *Prog Neurobiol* 55:257–332.
19. Pitkänen A (2000) in *The Amygdala: A Functional Analysis*, ed Aggleton JP (Oxford Univ Press, New York), pp 31–116.
20. Nelson RJ, Trainor BC (2007) *Nat Rev Neurosci* 8:536–546.
21. Franklin KBJ, Paxinos G (1997) *The Mouse Brain in Stereotaxic Coordinates* (Academic, New York).
22. Jones EG (1984) in *Cerebral Cortex: Cellular Components of the Cerebral Cortex*, eds Peters A, Jones EG (Plenum, New York), pp 521–552.
23. Morgan MA, Romanski LM, LeDoux JE (1993) *Neurosci Lett* 163:109–113.
24. Andersen P (1975) in *The Hippocampus*, eds Isaacson RL, Pribram KH (Plenum, New York), pp 155–175.
25. Amaral DG, Ishizuka N, Claiborne B (1990) *Prog Brain Res* 83:1–11.
26. Johnston D, Amaral DG (2004) in *The Synaptic Organization of the Brain*, ed Shepherd GM (Oxford Univ Press, New York), pp 455–498.
27. Winson J, Abzug C (1977) *Science* 196:1223–1225.
28. Acsady L, Kamondi A, Sík A, Freund T, Buzsáki G (1998) *J Neurosci* 18:3386–3403.
29. Freund TF, Buzsáki G (1996) *Hippocampus* 6:347–470.
30. Daumas S, Halley H, Francés B, Lassalle JM (2005) *Learn Mem* 12:375–382.
31. Rodriguez MA, Caruncho HJ, Costa E, Pesold C, Liu WS, Guidotti A (2002) *J Comp Neurol* 451:279–288.
32. Benes FM, Lange N (2001) *Trends Neurosci* 24:11–17.
33. Auta J, Chen Y, Ruzicka WB, Grayson DR (2007) in *Handbook of Neurochemistry and Molecular Neurobiology*, eds Baker G, Dunn S, Holt A, Lajtha A (Springer, New York), pp 341–361.